

# *Hoxc13* mutant mice lack external hair

Alan R. Godwin and Mario R. Capecchi<sup>1</sup>

Howard Hughes Medical Institute, Department of Human Genetics, University of Utah School of Medicine, Salt Lake City, Utah 84112-5331 USA

***Hox* genes are usually expressed temporally and spatially in a colinear manner with respect to their positions in the *Hox* complex. Consistent with the expected pattern for a paralogous group 13 member, early embryonic *Hoxc13* expression is found in the nails and tail. *Hoxc13* is also expressed in vibrissae, in the filiform papillae of the tongue, and in hair follicles throughout the body; a pattern that apparently violates spatial colinearity. Mice carrying mutant alleles of *Hoxc13* have been generated by gene targeting. Homozygotes have defects in every region in which gene expression is seen. The most striking defect is brittle hair resulting in alopecia (hairless mice). One explanation for this novel role is that *Hoxc13* has been recruited for a function common to hair, nail, and filiform papilla development.**

[Key Words: *Hox* genes; hair follicles; filiform papillae; hair keratins; gene targeting; nails]

Received September 19, 1997; revised version accepted October 24, 1997.

The *Hox* genes encode a set of evolutionarily conserved transcription factors. In mice and humans, there are 39 *Hox* genes arranged in four linkage groups (*HoxA-D*) on separate chromosomes. The mammalian organization of these genes appears to be the result of quadruplication that occurred early in vertebrate phylogeny of a single ancestral complex common to both vertebrates and invertebrates (Pendleton et al. 1993; Holland and Garcia-Fernandez 1996). On the basis of sequence similarities and location within the linkage groups, these genes have been placed into 13 paralogous groups (Scott 1992). In addition to sequence similarities, the temporal and spatial expression patterns of paralogous genes are often similar (Gaunt et al. 1989; Krumlauf 1994).

In general, the position of a gene within each complex determines the anterior limits of its expression. The 3' genes have the most anterior limits of expression, and the anterior expression boundaries of more 5' genes are progressively more posterior. This colinearity of expression boundaries and the position in the complex is conserved between mouse and fly (Akam 1989; Duboule and Dollé 1989; Graham et al. 1989). Not only is the major anteroposterior axis of the embryo patterned in this manner by *Hox* genes, but so are other secondary axes in specialized regions of the body including the limb (Dollé et al. 1989), gut (Roberts et al. 1995; Yokouchi et al. 1995), and genitalia (Dollé et al. 1991b). In addition, in mice there is temporal colinearity such that the 3' genes are expressed earliest and further 5' genes progressively later during embryonic development (Duboule 1994). Consistent with the model of spatial colinearity, targeted mutations in mice have revealed that *Hox* genes

regionalize the embryo along its major axes and that the phenotypes of a given *Hox* mutation are generally confined to the region expected from its position within a complex.

The goal of this work was to define the sites of *Hoxc13* expression and to generate *Hoxc13* mutants to examine the roles of this gene in development. Surprisingly, in addition to gene expression and genetic defects in the caudal region of the axial skeleton and in the most distal regions of the limb (the nails), *Hoxc13* is expressed, and loss of its function has phenotypic consequences, in regions not predicted from the published expression patterns or mutational analysis of paralogous genes (Dollé et al. 1991a, 1993; Haack and Gruss 1993; Fromental-Ramain et al. 1996; Zeltser et al. 1996). The expression of *Hoxc13* in facial vibrissae and in the filiform papillae of the tongue may indicate that spatial colinearity does not accurately describe *Hox* gene expression at later embryological stages. Previous studies had suggested that the expression patterns of *Hox* genes also show spatial and temporal colinearity in the skin (Bieberich et al. 1991; Kanzler et al. 1994). *Hoxc13*, however, is expressed in hair follicles throughout the body rather than being regionally restricted. *Hoxc13* mutants are able to produce hair, but it shatters at the skin surface throughout the body, resulting in hairless mice. Our results suggest that *Hoxc13* has been recruited for unique functions in hair and filiform papilla development.

## Results

### *Generation of *Hoxc13*<sup>neo</sup> and *Hoxc13*<sup>lacZ</sup> mutant alleles*

Two mutant alleles of *Hoxc13* were generated as described in Materials and Methods. The first contains a

<sup>1</sup>Corresponding author.  
E-MAIL mario.capecchi@genetics.utah.edu; FAX (801) 585-3425.

Pol II-neo cassette inserted into DNA sequence encoding the homeodomain and thereby disrupts the capacity of the encoded protein to bind to DNA. The second contains an in-frame insertion of the *lacZ* gene at the same site of the homeodomain. This mutation also disrupts DNA binding capacity of *Hoxc13* protein, but at the same time generates a reporter to allow monitoring of *Hoxc13* expression in heterozygous and homozygous mutant embryos and mice. Figure 1, B and C, show Southern transfer analysis of ES cell lines, and mutant mouse offspring carrying the *Hoxc13<sup>neo</sup>* and *Hoxc13<sup>lacZ</sup>* mutant alleles.

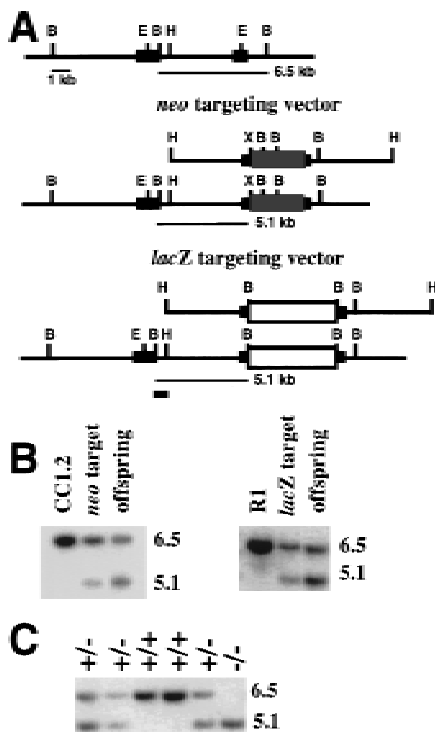


**Figure 1.** Targeting vectors and Southern blot analysis. (A) Genomic structure and targeting vectors. Large solid boxes represent *Hoxc13* exons, dark gray boxes the Pol II-neo cassette, the shaded boxes the *lacZ* MC1 *neo* cassette, (B) *Bam*HI, (E) *Eco*RI, (H) *Hind*III, and (X) *Xho*I. The position of the 5'-flanking probe used for Southern transfer analysis is indicated by the small solid box. The first line shows the wild-type genomic structure and subsequent lines show the *Hoxc13<sup>neo</sup>* and *Hoxc13<sup>lacZ</sup>* targeting vectors and the genomic structure resulting from homologous recombination. (B) Southern blot analysis of targeted cell lines and offspring from chimera generated from the targeted ES cell lines. The first three lanes show *Bam*HI-*Xho*I digests of the parental ES cell line CC1.2, a targeted ES cell line, and an offspring from a chimeric male. The second set of three lanes shows a *Bam*HI digest of DNA from the parental ES cell line R1, a targeted ES cell line, and an offspring from a chimeric male. (C) Genotype of a litter from a *Hoxc13<sup>neo</sup>* heterozygote intercross. Southern transfer analysis of *Bam*HI-*Xho*I-digested DNA was performed and shows two wild-type mice carrying only the 6.5-kb fragment, three heterozygous animals with both the 6.5- and 5.1-kb fragments, and one mutant homozygote with only the 5.1-kb fragment.

### Expression of *Hoxc13*

*Hoxc13* expression was monitored by  $\beta$ -galactosidase ( $\beta$ -gal) staining of heterozygous *Hoxc13<sup>lacZ</sup>* embryos and by RNA in situ hybridization in wild-type embryos. For embryonic day (E) 9.5 through E14.5, the  $\beta$ -gal expression pattern seen in the *Hoxc13<sup>lacZ</sup>* embryos was compared with RNA expression patterns in wild-type Swiss Webster embryos, and the expression patterns matched at each stage (e.g., Fig. 2C,D for E13.5). Because the  $\beta$ -gal staining is easier to detect and gives a higher signal-to-noise ratio, it, alone, is shown for the remaining embryonic stages. *Hoxc13* expression is first detected at E10.5 in the tail bud (Fig. 2A), and appears the same at E11.5 (data not shown). Expression continues in the tail at E12.5 but is also noted in the epithelia of the wrist and ankle areas (Fig. 2B). By E13.5, expression in the limb has become localized to the developing foot pads and nails (Fig. 2C), though it is still seen in the tail as reported earlier (Peterson et al. 1994). In addition, a striking pattern of expression is now detected in the vibrissae of the head. Expression is not limited to the primary and secondary vibrissae of the snout, but is seen also in the supraorbital and ulnarcarpal vibrissae. RNA in situ hybridization (Fig. 2D) confirms the E13.5  $\beta$ -gal staining pattern, as *Hoxc13* mRNA is detected in the vibrissae, tail, and very faintly in the developing nails. By E15.5, faint *Hoxc13* expression can be seen in a few hair follicles (data not shown). At E16.5, limb expression is limited to the nails. Furthermore, hair follicle expression is seen over the entire skin, and vibrissae expression appears weakened, possibly due to invagination of these follicles (see Fig. 2F). At E17.5, expression is detected in a second set of hair follicles arranged in circles surrounding the follicles that began expressing at E15.5 (Fig. 2G). In addition, the cilia (eyelashes) begin to express *Hoxc13* at this stage. The strongest digit expression becomes restricted to a single domain, whose shape resembles that of the adult nail (Fig. 2H).

The first pelage, or body coat hairs to form are the tylotrichs, a type of tactile hair. Their formation is initiated at E13.25 in the shoulders and is followed by a wave of follicle growth, simultaneously extending radially (i.e., caudally, anteriorly, ventrally, and dorsally) with completion of initiation between E15.25 and E16.25 (Mann 1962). Similarly, a wave of awl hair initiation starts in the shoulders at E16.25 and is completed by E18.25. Comparison of this developmental timing with *Hoxc13* expression data suggests that the first hair follicles to express *Hoxc13* at E15.5 will form tylotrichs and that the second set of expressing follicles at E17.5 will form awl hairs. This timetable also suggests that the first *Hoxc13* expression in hair follicles occurs ~1 day after initiation of the follicles. Similarly, vibrissae follicles are initiated between E12 and E12.5 (Mann 1962), and we first detect *Hoxc13* expression in vibrissae follicles at E13.5.

For each embryonic stage, the *Hoxc13* expression pattern in heterozygous and homozygous *Hoxc13<sup>lacZ</sup>* embryos was compared by use of  $\beta$ -gal staining (data not

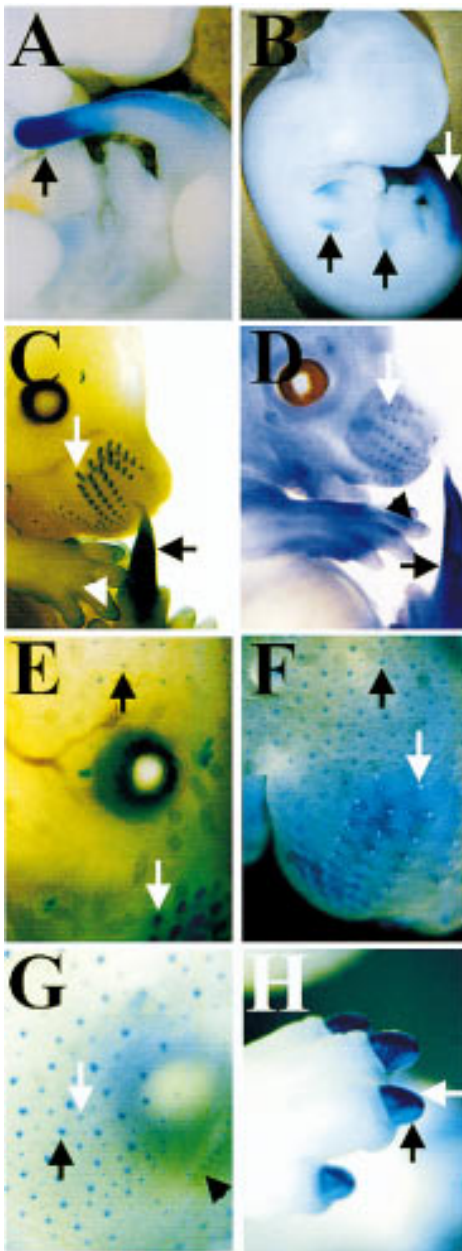


**Figure 2.** *Hoxc13* gene expression. (A–C,E–H)  $\beta$ -Gal staining of heterozygous *Hoxc13<sup>lacZ</sup>* embryos at the noted embryonic ages. D shows RNA in situ hybridization of a Swiss Webster embryo at E13.5. (A) E10.5 embryo. Tail expression is indicated by arrows. (B) E12.5 embryo. Black arrows show limb expression in wrist and ankle regions and white arrow shows tail expression. (C) E13.5 embryo. White arrow shows vibrissae expression; the black arrow shows tail expression; white arrowhead shows expression in a thin layer of the digits. (D) E13.5 embryo. White arrow shows vibrissae expression; black arrow shows tail expression; the black arrowhead shows faint digit expression. (E) E15.5 embryo. White arrow shows continuing vibrissae staining; black arrow shows beginning hair follicle expression. (F) E16.5 embryo. The white arrow shows lack of surface vibrissae expression; the black arrow shows hair follicle expression. (G) E17.5 embryo. The black arrow highlights hair follicle expression first seen at E15.5; the white arrow indicates expression in the second set of hair follicles. The black arrowhead indicates expression in the cilia. (H) E17.5 embryo. The white arrow indicates strong dorsal nail  $\beta$ -gal staining; the black arrow points to fainter ventral staining.

zygous mutant viability (~10% survive to adulthood). Newborn homozygotes of both alleles are easily identified, because they lack vibrissae at birth. Most homozy-

shown). The sites of *Hoxc13* expression were identical at each stage, although a more intense expression of  $\beta$ -gal was observed in homozygotes. The identical staining patterns in homozygotes and heterozygotes suggest that *Hoxc13* does not regulate its own transcription, contrary to what has been shown for several other *Hox* genes (Zappavigna et al. 1991; Pöpperl et al. 1995).

#### *Hoxc13* phenotypes

Animals heterozygous for either *Hoxc13* mutant allele appeared outwardly indistinguishable from wild-type mice (Fig. 3A,B) and were intercrossed to generate homozygotes. Both mutant alleles show a reduction of homo-

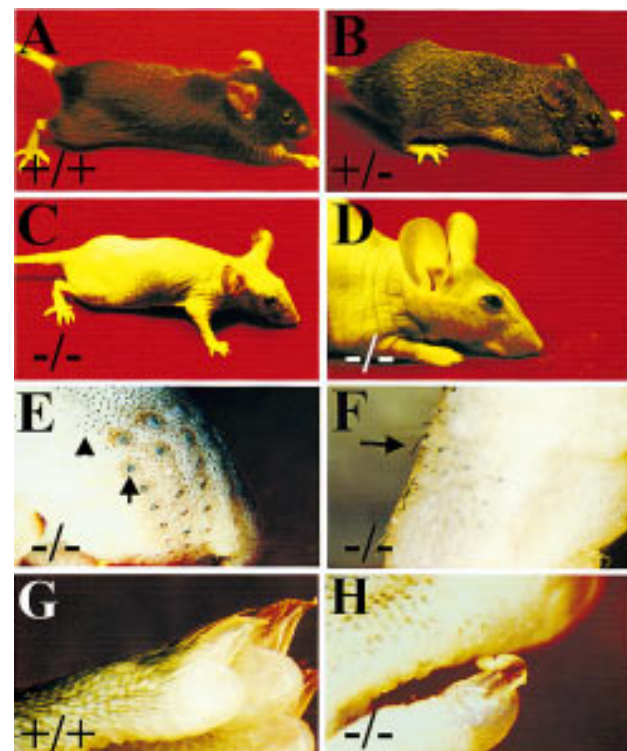


**Figure 3.** Overt *Hoxc13* phenotypes. (A) *Hoxc13<sup>neo</sup>* wild-type non-Agouti mouse. (B) *Hoxc13<sup>neo</sup>* heterozygous Agouti mouse. (C) *Hoxc13<sup>neo</sup>* homozygote. (D) Close-up of *Hoxc13<sup>neo</sup>* homozygote head. (E) Close-up of *Hoxc13<sup>neo</sup>* homozygote face. The black arrow shows lack of protruding vibrissae; the black arrowhead shows hair remnants under skin surface. (F) Close-up of *Hoxc13<sup>neo</sup>* homozygote lower limb. The black arrow shows rare protruding hair. (G) Wild-type nails. (H) Nails from a *Hoxc13<sup>neo</sup>* homozygote.

gotes die between postnatal day (P) 7 and 14. They show progressive weight loss and weakness relative to their littermates, suggesting a nutritional or metabolic problem. The reason for postnatal lethality is currently under examination.

Individuals that survive >2 weeks are fertile, healthy, and after weaning slowly approach the weight of their nonmutant siblings. The most striking phenotype of adult mutant mice is an absence of all pelage (or coat) hair types (see Fig. 3C), peri-anal hairs, cilia (eyelashes), and all vibrissae (Fig. 3D,E). Indeed, all hair types described to date in the mouse (Sundberg and Hogan 1994) appear to be affected in *Hoxc13* mutants. Whereas the tail hairs are missing, the tail scales appear unaffected under gross observation. Close examination of the skin of homozygotes reveals that the pelage hair forms, but is fractured at the skin surface (see Fig. 3E). In rare instances, hair can be found protruding from the epidermis in protected regions (especially along the lower limbs, Fig. 3F). Occasionally, in-grown hairs are observed within the epidermis. Finally, the nails of homozygotes are malformed, having a flatter appearance, and are often twisted (Fig. 3H) when compared with wild-type nails (Fig. 3G).

#### Hair expression

The overt hair phenotype as well as the whole-mount detection of *Hoxc13* expression in hair follicles led us to examine the expression of *Hoxc13* in this region in greater detail. As shown in Figure 4A, *Hoxc13* gene expression in skin continues after birth until at least P14. Higher magnification shows lack of *Hoxc13* expression in the dermal papillae of the hair follicles (data not shown). As a hair follicle cell type marker, we used an antibody against an epidermal type II keratin intermediate filament protein [keratin 6 (K2.6)], which specifically labels a layer of cells termed the companion cells, but doesn't stain the inner root sheath or noninduced outer root sheath cells (Rothnagel and Roop 1995). By double-labeling of *Hoxc13<sup>lacZ</sup>* heterozygotes and homozygotes for  $\beta$ -gal activity and anti-K2.6 antibody, we were able to localize *Hoxc13* expression in hair follicles. In both homozygotes and heterozygotes, the rapidly dividing and differentiating keratinocytes directly above the dermal papilla express *Hoxc13* (Fig. 4B for homozygotes). In addition, *Hoxc13* expression (blue) is colocalized in the nuclei of a single cell layer that also expresses K2.6 (brown staining) (Fig. 4C). Thus, *Hoxc13* appears to be expressed in the companion layer. The only difference noted between heterozygous (data not shown) and homozygous mutant hair follicles was the intensity of  $\beta$ -gal staining. The companion layer is present in mutant homozygotes and appears morphologically normal.

#### *Hoxc13* in filiform papillae

Filiform papillae are structures on the dorsal surface of the tongue. The spine region of the filiform papillae is especially variant in shape between mammalian species,

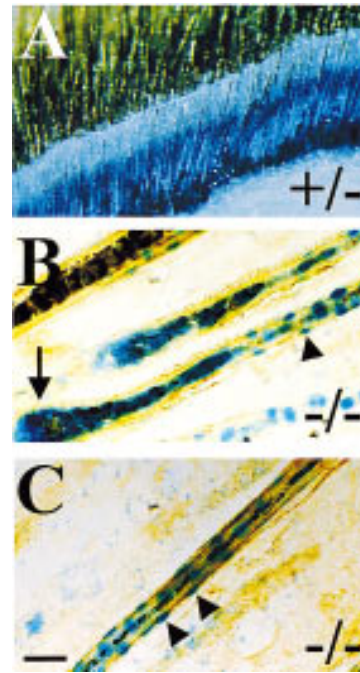


**Figure 4.** *Hoxc13* expression in the hair and histology. (A)  $\beta$ -Gal staining of postnatal day (P) 7 skin of *Hoxc13<sup>lacZ</sup>* heterozygote. (B)  $\beta$ -Gal staining (blue) and anti-K2.6 immunohistochemistry (brown) of *Hoxc13<sup>lacZ</sup>* homozygous skin. The black arrow shows expression in rapidly dividing keratinocytes; the black arrowhead shows expression in single nuclei in companion layer. (C)  $\beta$ -Gal staining and anti-K2.6 immunohistochemistry of *Hoxc13<sup>lacZ</sup>* homozygous skin. Black arrowheads indicate nuclear staining in nuclei of the companion layer. Scale bar, 20  $\mu$ m (shows magnification for B and C).

reflecting specialized uses of the tongue (Dhouailly et al. 1989). In mice, the filiform papilla spines resemble sharply curved talons that point posteriorly (see Fig. 6A, below). Skin, esophageal, and hair keratins are differentially expressed on the dorsal surface of the tongue (Dhouailly et al. 1989). Resemblance to hair follicles is suggested by the presence of a dermal papillae-equivalent in filiform papillae and reaction in the spine region of filiform papillae of an antibody (AE14) specific for late hair cortex differentiation (Dhouailly et al. 1989). The hair keratin intermediate filament genes *mHa3*, *mHb3*, and *mHb4* are expressed in a posterior compartment of the filiform papillae extending into the spine (Tobiasch et al. 1992; Winter et al. 1994).

*Hoxc13* is expressed in the tongue, specifically in the filiform papillae, at least as early as E17.5 (data not shown; see Fig. 5A for an example at P6). Each filiform papilla also expresses *Hoxc13* postnatally. The gaps in expression (white circles) show that the fungiform papillae, a type of taste bud scattered along the tongue surface, do not express *Hoxc13*.  $\beta$ -Gal staining followed by histological examination revealed that *Hoxc13* is expressed primarily in the base of the filiform papillae, although low levels of expression are seen in the keratinized spine (see especially the homozygote sections Fig. 5D,H). The region of *Hoxc13* expression appears to cor-

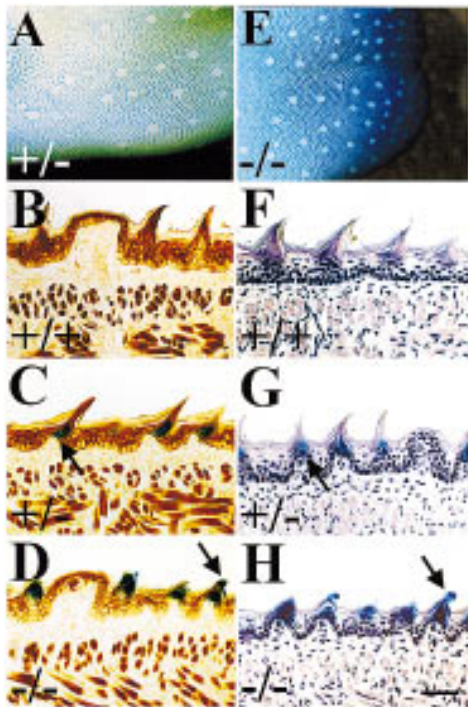


**Figure 5.** Tongue expression and histology. (A,E)  $\beta$ -Gal staining of P6 tongues from a *Hoxc13<sup>lacZ</sup>* heterozygote and homozygote, respectively. (B–D)  $\beta$ -Gal staining (blue) and anti-K2.6 immunohistochemistry (brown) on P6 tongues, whereas F–H show  $\beta$ -gal staining and hematoxylin–eosin staining. H&E staining was performed as described previously (Mansour et al. 1993). Scale bar, (H), 50  $\mu$ m (shows the magnification for B–D and F–H). B and F are of wild-type sections, C and G from a *Hoxc13<sup>lacZ</sup>* heterozygote, and D and H from a *Hoxc13<sup>lacZ</sup>* homozygote. Arrows in C and G indicate  $\beta$ -gal staining in the base of the spines. Arrows in D and H show  $\beta$ -gal staining extending into the malformed spines.

respond closely to that determined for hair keratins, especially *mHa3* (Winter et al. 1994). Colocalization of the X-gal precipitate (blue) and the diaminobenzidine K2.6 immunohistochemical product (brown) shows that the *Hoxc13* expression domain is within a subset of the K2.6 expression domain (Fig. 5C). In mutant homozygotes, the filiform papillae appear more rounded than in heterozygotes and the  $\beta$ -gal staining is closer to the surface, suggesting that the mutant phenotype is already manifest at P6 (Fig. 5D,H).

Scanning electron microscopy was used to examine the filiform papillae of adults in greater detail (Fig. 6). Although sets of littermates of different ages were used, no age-related differences were noted. All wild-type and heterozygous *Hoxc13* mice had the characteristic talon-shaped filiform papillae, whereas in all homozygotes the spines appeared to have broken off. Examination of the surface of the tongues of homozygotes revealed broken pieces of filiform papilla spines lying on the surface in some microscopic views (Fig. 6C). The presence of these broken pieces suggests that, even though the mutant phenotype was seen histologically at P6 (Fig. 5D,H), some outgrowth of filiform papillae must eventually oc-

cur. Broken pieces were seen very infrequently on the tongues of heterozygous or wild-type mice. Thus, as for the hair phenotype, *Hoxc13* mutants appear to form weakened filiform papillae that shatter during usage. Fungiform papillae, in which *Hoxc13* is not expressed, appear normal in the homozygous mutants and the overall shape of the tongue is normal.

#### Skeletal phenotype

Adult *Hoxc13* homozygotes were examined for axial and appendicular skeleton defects. No evident appendicular skeleton defects were found, but homozygotes and heterozygotes showed an increase in the number of caudal vertebrae with lateral processes. Wild-type mice have four sacral vertebrae followed by four or five caudal vertebrae with lateral processes and a variable number of caudal vertebrae without lateral processes (see Fig. 7A). Most heterozygotes had six or seven caudal vertebrae with lateral processes (Fig. 7B), whereas homozygotes had 10 to 13 caudal vertebrae with lateral processes (Fig. 7C). When the total number of caudal vertebrae in mutant homozygotes were counted, however, the range was the same as that for wild-type mice (28–32; Grüneberg 1955). Because the number of altered vertebrae in mutant animals is larger than the difference in total number of caudal vertebrae seen between individuals in both wild-type and mutant mice (four vertebrae), a true homeotic transformation is suggested.

#### Discussion

We have shown that *Hoxc13* has an unexpected expression pattern relative to published reports of the expression patterns of its paralogous genes. Moreover, mice that carry targeted mutations of *Hoxc13* exhibit defects in the body areas in which expression is found. The gene expression patterns between E9.5–E14.5 were determined by both a targeted LacZ protein fusion in heterozygotes, as well as an RNA in situ probe on wild-type embryos. For each embryonic stage that was compared, identical expression patterns were found with the two techniques. *Hoxc13* is first expressed in the tail beginning at E10.5, followed by expression in the limb begin-

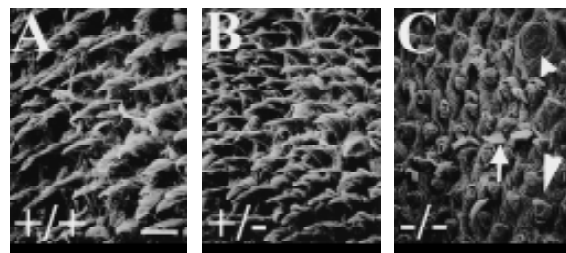


**Figure 6.** Scanning electron micrographs of adult tongues. Scale bar in A is 50  $\mu$ m (A–C). (A) Wild-type tongue. (B) *Hoxc13<sup>lacZ</sup>* heterozygote tongue. (C) *Hoxc13<sup>lacZ</sup>* homozygote tongue. The small white arrowhead shows a fungiform papilla; the large white arrowhead shows a filiform papilla remnant; the white arrow shows a broken-off filiform papilla piece on the tongue surface.



**Figure 7.** Axial skeleton phenotype. (A) Wild-type skeleton. (B) *Hoxc-13<sup>neo</sup>* heterozygote skeleton. (C) *Hoxc-13<sup>neo</sup>* homozygote skeleton. (S1) represents sacral vertebra 1, (S4) sacral vertebra 4, and (C1) caudal vertebra 1. In addition, the last caudal vertebra with a lateral projection is labeled for each genotype (i.e., caudal vertebra C5 in A). Preparation of skeletons was as described previously (Davis and Capecchi 1994).

ning at E12.5. The expression in the limb appears to be ectodermal. These expression patterns for *Hoxc13* were predictable from the expression patterns of group 13 paralogs as well as from phenotypic analysis of animals carrying mutations in these paralogs. For example, *Hoxa13* and *Hoxd13* are expressed not only in the spinal cord and prevertebrae, but also in the limb, genital tubercle, and hindgut (Dollé et al. 1991a; Haack and Gruss 1993; Roberts et al. 1995; Yokouchi et al. 1995). Targeted and spontaneous mutations in these *Hox* genes severely affect autopod development in the limb as well as affecting the urogenital system (Dollé et al. 1993; Kondo et al. 1996; Mortlock et al. 1996; Goodman et al. 1997; Mortlock and Innis 1997). The recently discovered *Hoxb13* gene is expressed in the posterior hindgut anterior to the anal canal and in the urogenital sinus of the urogenital tract (Zeltser et al. 1996).

The expression patterns and mutant phenotypes for the paralogs of *Hoxc13* suggest that limb, hindgut, and urogenital expression domains were reasonable expectations for *Hoxc13*. Beginning at E13.5, however, a strikingly different *Hoxc13* expression pattern begins in the developing vibrissae. This vibrissal expression encompasses all classes of vibrissae: the primary vibrissae in the snout as well as the secondary vibrissae, including the supraorbital and ulnar–carpal vibrissae. Expression of *Hoxc13* begins in a few developing hair follicles at E15.5, and by E16.5 has spread to follicles throughout the body. A second set of hair follicles, destined to form awl hairs,

begins expressing *Hoxc13* at E17.5, and expression in the hair continues until at least 2 weeks after birth. In hair, *Hoxc13* expression colocalizes with keratin 6 expression to a single cell layer, the companion layer, in the root sheath. In addition, *Hoxc13* is expressed in the rapidly dividing keratinocytes in the hair bulb and expression extends into the hair shaft. *Hoxc13* is also expressed postnatally in the developing filiform papillae of the tongue.

*Hoxc13* mutants have defects corresponding to the sites of expression we have described. *Hoxc13* heterozygotes and homozygotes both have additional caudal vertebrae with lateral processes as compared with wild-type mice. Up to 7 caudal vertebrae in the heterozygotes and up to 13 caudal vertebrae in the mutant homozygotes have lateral processes, compared with a maximum of 5 caudal vertebrae with lateral processes in wild-type mice. *Hoxd13* mutations affect the axial skeleton in a similar but more anterior region, because in these mutants sacral vertebra four is altered to resemble sacral vertebra three and caudal vertebra one is transformed to resemble sacral vertebra four (Dollé et al. 1993). Thus, a phenotype in this region of the axial skeleton was expected from studies of paralogs. In addition, axial skeleton alterations have become one of the most common phenotypes detected in *Hox* mutants (for review, see Boulet and Capecchi 1996).

Similar to both *Hoxa13* and *Hoxd13* mutants, *Hoxc13* mutants also show an alteration in the limb. Whereas both *Hoxa13* and *Hoxd13* mutants have alterations in the phalanges as well as other limb bones, however, the limb defects of *Hoxc13* mutants are restricted to the nails, which are derived from ectoderm. In *Hoxc13* mutant homozygotes, the nails are flatter compared with the talon-shaped nails of wild-type mice and often overgrow, forming long spirals. Because many of the proteins found in nails are also found in the tongue and hair (e.g., Lynch et al. 1986; Heid et al. 1988), it is possible the nail phenotype does not correspond to patterning of the limb per se, but instead, reflects a role for *Hoxc13* discussed below.

In addition to the defects discussed thus far, *Hoxc13* homozygotes have deficiencies in hair, vibrissae, and the filiform papillae of the tongue that appear to be related to one another. Indeed, all the major sites of trichocytic (or hard) keratin appear to be affected in *Hoxc13* mutants (Heid et al. 1988). Close examination of the skin of mutant homozygotes reveals subdermal hair that appears to have shattered at the surface. In regions of the body, such as the lower limb, which are rubbed less frequently, hair that protrudes above the body surface is occasionally found. In addition, rare in-grown hairs can be detected below the skin surface. Similarly, electron micrographs of tongues of homozygotes reveal not only jagged edges on the remnants of the filiform papillae, but also shattered pieces of the filiform papillae lying on the tongue surface. A plausible explanation for these hair and filiform papillae defects is that the production of structural proteins required both for hair and for the spine region of filiform papillae is regulated directly or indirectly by

*Hoxc13*. During evolution, *Hoxc13* may have been recruited into a role specific for hair genes, which has resulted not only in regulation of a structural gene for hair development, but also in regulation of the same gene(s) or related genes in vibrissae, nail, and filiform papillae.

An alternative explanation for the *Hoxc13* phenotype is that the neomycin gene in our targeted mutations affects expression of a neighboring keratin gene. However, several lines of evidence suggest that this is not the case. First, although the keratin 2 complex (*Krt-2*), which contains both the epidermal and hair type II keratin intermediate filament genes (Compton et al. 1991; Powell and Rogers 1997), is linked to the *HoxC* complex on mouse chromosome 15, the two complexes are at least 1.3 cM apart [Mouse Genome Database (MGD), Mouse Genome Informatics, The Jackson Laboratory, Bar Harbor, ME. World Wide Web URL: <http://www.informatics.jax.org>; July, 1997]. In addition, in a *Mus spretus* X *Mus musculus* cross, one recombinant between the *HoxC* and *Krt-2* complexes was observed in 50 meioses tested (Hart et al. 1992). Thus, the *neo* gene is likely to be too far from the *Krt-2* control elements to affect its expression. Most importantly, *Hoxc13* RNA is detected in the same pattern in wild-type embryos as the  $\beta$ -gal pattern in *Hoxc13<sup>lacZ</sup>* embryos. The presence of *Hoxc13* transcripts in nails, filiform papillae, vibrissae, and hair strongly suggests that mutation of *Hoxc13* alone could account for the observed phenotypes. A simpler explanation is that *Hoxc13* has adopted a role controlling gene products common to a differentiated state in each of these body regions. This suggests a novel role for *Hox* genes in differentiated tissues, namely, the regulation of the production of structural proteins specific to a given differentiated state.

The hair keratin intermediate filament genes and keratin-associated protein genes are primary candidates for being downstream targets of *Hoxc13*. Hair phenotypes similar to that of *Hoxc13* mutants have been obtained by overexpression of individual keratin intermediate filament genes in transgenic mice. Overexpression of a mouse epidermal type II keratin intermediate filament (K2.6) gene resulted in transgenic mice that developed alopecia at 6 months (Rothnagel and Roop 1995). Expression of a sheep wool intermediate filament keratin gene in the hair cortex in transgenic mice caused cyclic hair loss (Powell and Rogers 1990). In addition, misexpression and overexpression of a keratin-associated protein under the promoter of a type II hair keratin intermediate filament gene resulted in transgenic mice with brittle hair, which broke off giving a naked appearance (Rogers and Powell 1993). Finally, the human inherited hair disease monilethrix, which manifests as hair prone to breakage, is caused by mutations in the the hair cortex keratin hHb6 (Winter et al. 1997).

Although expression of the epidermal type II keratin K2.6 gene was not affected in *Hoxc13* homozygotes, it has been shown that eight major and two minor hair keratin intermediate filament genes exist in mouse (Heid et al. 1986; Lynch et al. 1986; Winter et al. 1997) and ~60 hair keratin associated protein genes may exist

(Powell and Rogers 1997), leaving many potential candidate target genes. There are two general schemes by which *Hoxc13* could be affecting keratin expression. Because *Hoxc13* is expressed in the developing nail, the base of the spine of filiform papillae, and in the rapidly dividing keratinocytes of the hair follicles, *Hoxc13* could directly control the transcription of hair keratin genes. Alternatively, at least for the hair follicle, because the keratinocytes rapidly differentiate and proceed into different developmental pathways (Fuchs 1995; Powell and Rogers 1997), *Hoxc13* could control proliferation of, or differentiation into, cell types specific for one or more of these pathways and, thus, secondarily affect keratin expression. *Hox* genes have been proposed previously to control proliferation of cells in chondrogenic centers for bone formation in limb (Davis and Capecchi 1994; Duboule 1994) and cervical vertebrae (Condie and Capecchi 1994).

A hallmark of *Hox* gene expression studies has been the relationship of position within a complex and the region of expression along the anteroposterior axis of an embryo. Spatial colinearity with respect to the anteroposterior body axis is conserved between flies and mammals and in mammalian development it is also observed within certain organs or body parts, such as the genital tract, gut, and limb. It should be stressed that the early expression pattern of *Hoxc13*, E10.5–E12.5, does reflect the spatial and temporal characteristic common to group 13 paralogous members, and only the subsequent expression in the hair follicles and filiform papillae departs from the spatial colinearity model. Newborn and adult expression patterns are not known in detail for many *Hox* genes. In addition, many *Hox* mutants die during the first critical time period for which the *Hox* gene is required, for example at birth as a result of esophageal defects (Boulet and Capecchi 1996). Thus, potential adult phenotypes of many of these mutants are impossible to ascertain without the use of conditional mutations. Our finding that later *Hoxc13* expression does not conform to spatial colinearity suggests that late expression patterns for additional *Hox* genes need to be examined to determine the generality of spatial colinearity, or lack thereof, in late development and in adulthood.

There are other cases where *Hox* genes appear to be expressed in tissues that may contradict spatial colinearity. For example, *Hox* expression is seen in restricted hematopoietic lineages (Lawrence et al. 1996; Zimmerman and Rich 1997). With respect to the expression of *Hox* genes in blood cells, however, mutational analysis has not yet uncovered a clear role for *Hox* gene function in hematopoiesis.

RNA in situ hybridization has shown regionally-restricted expression of *Hoxc8*, *Hoxd9*, *Hoxd11*, and *Hoxd13* in skin, suggesting spatial colinearity of *Hox* expression in this tissue. By RNA in situ hybridization, as well as by examination of the expression pattern of a *Hoxc8* enhancer-driven *lacZ* transgene, *Hoxc8* expression was found to be restricted dorsally to the lumbar region, whereas expression was seen from throat to tail in more ventral regions of the body (Bieberich et al. 1991;

Kanzler et al. 1994). Not only the mesenchymally-derived dermis and dermal papillae, but also the epithelial-derived portions of the hair follicle and epidermis express *Hoxc8*. In contrast, *Hoxd9*, *Hoxd11*, and *Hoxd13* are restricted to the caudal region and are only expressed in the epithelial-derived portions of the hair follicle (Kanzler et al. 1994). Similarly, expression of *Hoxc6* and *Hoxd9* in chick feather buds shows body surface restrictions (Choung et al. 1990). Many other *Hox* genes have been found to be expressed in skin by PCR methods, but spatial expression information is still lacking. *Hoxc13* does not conform to the apparent spatial colinearity of position in a *Hox* complex and expression pattern in the skin, because it is expressed in hair follicles throughout the body. Expression studies for *Hoxc4* and *Hoxb6* suggest they may also be globally expressed (Matthews et al. 1993; Rieger et al. 1994). *Hoxc13* is, however, restricted to the epithelial-derived hair follicle regions, similar to the *HoxD* genes just discussed above.

In summary, we have shown that mice mutant for *Hoxc13* have defects in hair, vibrissae, nail, and filiform papilla development as well as in caudal vertebrae. The *Hoxc13* gene is expressed in each of these areas, even those well outside the area expected for a paralogous group 13 gene, suggesting that the defects seen in each of these regions are defects directly attributable to a developmental program controlled by *Hoxc13*. Although other *Hox* genes have been shown to be expressed in hair, *Hoxc13* is the first *Antennapedia*-class homeobox gene shown to have overt phenotypic effects on hair development. This is also the first *Hox* mutant to suggest that *Hox* genes can control not only proliferation and differentiation but also structural protein synthesis. Finally, *Hoxc13* is unlikely to be the only mammalian *Hox* gene co-opted for additional developmental roles. Thus, many new exciting roles for *Hox* genes late in development or in adulthood may remain to be discovered.

## Materials and methods

### Targeted mutagenesis of *Hoxc13*

A CC1.2 ES cell line-derived genomic phage  $\lambda$  library was screened for *Hoxc13* by use of an oligonucleotide, 5'-TACCTG-GCGCTCAGAGAGGTTTCGTGGTGGCGGAGATGCGCCG-3', derived from the human *Hoxc13* sequence (Acampora et al. 1989). A 10-kb *HindIII* fragment was isolated from this phage for use in the targeting vector. A replacement vector was generated by insertion of the *Pol II-neo* cassette (Deng et al. 1993) at a unique *BstEII* site in the sequence encoding the third helix of the homeodomain. This fragment was then ligated between the TK1 and TK2 genes in a phage vector. The vector was electroporated into CC1.2 cells (Bradley et al. 1984) and positive-negative selection was applied (Mansour et al. 1988). One quarter of the lines tested (27/108) had undergone homologous recombination, which was verified with a 5'-flanking probe, a 3'-flanking probe, and an internal *neo* probe (data not shown). Cell lines that had undergone homologous recombination were microinjected into C57Bl/6 blastocysts to generate chimeric males.

The *lacZ* fusion vector was generated by insertion of an *XhoI* linker into the same *BstEII* site followed by in-frame insertion of *lacZ* (Mansour et al. 1990). The *lacZ* vector was

electroporated into R1 cells (Nagy et al. 1993) and positive-negative selection was applied. Six of 66 cell lines had undergone homologous recombination, which was confirmed by use of all three probes as described above.

### Genotyping

DNA from newborn or adult tail or skin biopsies as well as DNA from embryonic yolk sacs was isolated as described previously (Thomas et al. 1992). Genotypic analysis was performed by Southern blotting with *Bam*HI plus *Xho*I digestion for the *Hoxc13<sup>neo</sup>* allele and *Bam*HI digestion for the *Hoxc13<sup>lacZ</sup>* allele and probing with a 500-bp *Bam*HI-*Hind*III probe (see Fig. 1). All alleles are distinguishable by *Bam*HI digestion of DNA, because the *Hoxc13<sup>neo</sup>* allele, when hybridized with the probe described above, shows a 5.6-kb fragment, whereas the *Hoxc13<sup>lacZ</sup>* allele has a 5.1-kb fragment, and the wild-type allele has a 6.5-kb fragment. A representative Southern transfer analysis for a *Hoxc13<sup>neo</sup>* intercross is shown in Figure 1C.

### RNA in situ hybridization

Whole mount RNA in situ hybridization was performed as described previously (Carpenter et al. 1993) with a 362-bp probe derived from the *Hoxc13* 3' untranslated region beginning one bp 3' of the UGA stop codon.

### $\beta$ -Gal staining and keratin 2.6 immunohistochemistry

$\beta$ -Gal staining was performed overnight as described previously (Mansour et al. 1993), except times of fixation were optimized for each embryonic stage and tissue, and reactions were carried out at 30°C. For the keratin 6 detection postfixation was performed as described previously (Fekete 1938). Specimens were dehydrated, embedded in Paraplast X-tra (CMS), and sections of 10  $\mu$ m were collected. Sections were dewaxed, rehydrated, washed in PBS, blocked with 3% goat serum in PBS, reacted with keratin 6 antibody (kindly provided by D. Roop, Baylor College of Medicine, Houston, TX) diluted 1:500 in 3% goat serum in PBS, washed with PBS, and reacted with donkey anti-rabbit HRP-conjugated secondary antibody (Jackson ImmunoResearch Laboratories) at 1:300 in 3% goat serum in PBS. After washing with PBS, the sections were reacted with 0.5 mg/ml of DAB (Sigma) with 0.3% H<sub>2</sub>O<sub>2</sub> in PBS for 15 min. Color reactions were halted by PBS washes, the sections were dehydrated, and coverslips were mounted by use of D.P.X. (Aldrich).

### Scanning electron microscopy

Adult and weaning-age tongues were fixed in the dark in a 1% aqueous osmium tetroxide solution (Polysciences, Inc.) for 4 hr, rinsed, dehydrated in ethanol, critical point dried, and sputter-coated with a 60/40 gold/palladium alloy. Specimens were placed on mounts by use of double-stick tape and examined in a Hitachi S-450 scanning electron microscope at a working distance of 15 mm at 15 kV and a magnification of 300 $\times$ . Images were recorded on Polaroid 55 P/N film. Microscopy was performed on three wild-type mice, two *Hoxc13<sup>neo</sup>* heterozygotes, four *Hoxc13<sup>lacZ</sup>* heterozygotes, one *Hoxc13<sup>neo</sup>* homozygote, and five *Hoxc13<sup>lacZ</sup>* homozygotes.

## Acknowledgments

We thank C. Lenz, M. Allen, and G. Peterson for expert technical assistance. We are grateful to J. Sundberg, J. Andreoli, K. Stenn, and members of the Capecchi laboratory for suggestions

during the course of these experiments. We thank D. Roop for graciously providing the keratin 6 antibody, E. King and the Imaging Facility in the Department of Biology for assistance with scanning electron microscopy, and L. Oswald for help in the preparation of the manuscript. A.R.G. was supported by an American Cancer Society postdoctoral fellowship (PF-3863). He was also an associate of the Howard Hughes Medical Institute.

The publication costs of this article were defrayed in part by payment of page charges. This article must therefore be hereby marked "advertisement" in accordance with 18 USC section 1734 solely to indicate this fact.

## References

- Acampora, D., M. D'Esposito, A. Faiella, M. Pannese, E. Migliaccio, F. Morelli, A. Stornaiolo, Y. Nigro, A. Simeone, and E. Boncinelli. 1989. The human hox gene family. *Nucleic Acids Res.* **17**: 10385-10402.
- Akam, M. 1989. *Hox* and *HOM*: Homologous gene clusters in insects and vertebrates. *Cell* **57**: 347-349.
- Bieberich, C.J., F.H. Ruddle, and K.S. Stenn. 1991. Differential expression of the *Hox 3.1* gene in adult mouse skin. *Ann. N.Y. Acad. Sci.* **642**: 346-353.
- Boulet, A.M. and M.R. Capecchi. 1996. Targeted disruption of *hoxc-4* causes esophageal defects and vertebral transformations. *Dev. Biol.* **177**: 232-249.
- Bradley, A., M. Evans, M.H. Kaufman, and E. Robertson. 1984. Formation of germ-line chimaeras from embryo-derived teratocarcinoma cell lines. *Nature* **309**: 255-256.
- Carpenter, E.M., J.M. Goddard, O. Chisaka, N.R. Manley, and M.R. Capecchi. 1993. Loss of *Hox-A1* (*Hox-1.6*) function results in the reorganization of the murine hindbrain. *Development* **118**: 1063-1075.
- Choung, C.-M., G. Oliver, S.A. Ting, B.G. Jegalian, H.M. Chen, and E.M. de Robertis. 1990. Gradients of homeoproteins in developing feather buds. *Development* **110**: 1021-1030.
- Compton, J.G., D.M. Ferrara, D.-W. Yu, V. Recca, I.M. Freedberg, and A.P. Bertolino. 1991. Chromosomal localization of mouse hair keratin genes. *Ann. N.Y. Acad. Sci.* **642**: 32-43.
- Condie, B.G. and M.R. Capecchi. 1994. Mice with targeted disruptions in the paralogous genes *hoxa-3* and *hoxd-3* reveal synergistic interactions. *Nature* **370**: 304-307.
- Davis, A.P. and M.R. Capecchi. 1994. Axial homeosis and appendicular skeleton defects in mice with a targeted disruption of *hoxd-11*. *Development* **120**: 2187-2198.
- Deng, C., K.R. Thomas, and M.R. Capecchi. 1993. Location of crossovers during gene targeting with insertion and replacement vectors. *Mol. Cell. Biol.* **13**: 2134-2140.
- Dhouailly, D., C. Xu, M. Manabe, A. Schermer, and T.-T. Sun. 1989. Expression of hair-related keratins in a soft epithelium: Subpopulations of human and mouse dorsal tongue keratinocytes express keratin markers for hair-, skin-, and esophageal-types of differentiation. *Exp. Cell Res.* **181**: 141-158.
- Dollé, P., J.-C. Izpisua-Belmonte, H. Falkenstein, A. Renucci, and D. Duboule. 1989. Coordinate expression of the murine *Hox-5* complex homeobox-containing genes during limb pattern formation. *Nature* **342**: 767-772.
- Dollé, P., J.-C. Izpisua-Belmonte, E. Boncinelli, and D. Duboule. 1991a. The *Hox-4.8* gene is localized at the 5' extremity of the *Hox-4* complex and is expressed in the most posterior parts of the body during development. *Mech. Dev.* **36**: 3-13.
- Dollé, P., J.-C. Izpisua-Belmonte, J.M. Brown, C. Tickle, and D. Duboule. 1991b. *Hox-4* genes and the morphogenesis of mammalian genitalia. *Genes & Dev.* **5**: 1767-1777.
- Dollé, P., A. Dierich, M. LeMeur, T. Schimmang, B. Schuhbaur, P. Chambon, and D. Duboule. 1993. Disruption of the *Hoxd-13* gene induces localized heterochrony leading to mice with neotenic limbs. *Cell* **75**: 431-441.
- Duboule, D. 1994. Temporal colinearity and the phylotypic progression: A basis for the stability of a vertebrate Bauplan and the evolution of morphologies through heterochrony. *Development* (Suppl.) 135-142.
- Duboule, D. and P. Dollé. 1989. The structural and functional organization of the murine *Hox* gene family resembles that of *Drosophila* homeotic genes. *EMBO J.* **8**: 1497-1505.
- Fekete, E. 1938. A comparative morphologic study of the mammary gland in a high and low tumor strain of mice. *Am. J. Pathol.* **14**: 557-578.
- Fromental-Ramain, C., X. Warot, N. Messadecq, M. LeMeur, P. Dollé, and P. Chambon. 1996. *Hoxa-13* and *Hoxd-13* play a crucial role in the patterning of the limb autopod. *Development* **122**: 2997-3011.
- Fuchs, E. 1995. Keratins and the skin. *Annu. Rev. Cell Dev. Biol.* **11**: 123-153.
- Gaunt, S.J., R. Krumlauf, and D. Duboule. 1989. Mouse homeo-genes within a subfamily, *Hox-1.4*, *-2.6* and *-5.1* display similar anteroposterior domains of expression in the embryo, but show stage- and tissue-dependent differences in their regulation. *Development* **107**: 131-141.
- Goodman, F.R., S. Mundlos, Y. Muragaki, D. Donnai, M.L. Giovannucci-Uzielle, E. Lapi, F. Majewski, J. McGaughran, C. McKeown, W. Reardon, J. Upton, R.M. Winter, B.R. Olsen, and P.J. Scambler. 1997. Synpolydactyly phenotypes correlate with size of expansions in HOXD13 polyalanine tract. *Proc. Natl. Acad. Sci.* **94**: 7458-7463.
- Graham, A., N. Papalopulu, and R. Krumlauf. 1989. The murine and *Drosophila* homeobox gene complexes have common features of organization and expression. *Cell* **57**: 367-378.
- Grüneberg, H. 1955. Genetical studies on the skeleton of the mouse XVII. Bent-tail. *J. Genet.* **53**: 551-562.
- Haack, H. and P. Gruss. 1993. The establishment of murine *Hox-1* expression domains during patterning of the limb. *Dev. Biol.* **157**: 410-422.
- Hart, C.P., J.G. Compton, S.H. Langley, L. Hunihan, K.P. LeClair, A. Zelent, T.H. Roderick, and F.H. Ruddle. 1992. Genetic linkage analysis of the murine developmental mutant velvet coat (*Ve*) and the distal chromosome 15 developmental genes *Hox-3.1*, *Rar-gamma*, *Wnt-1*, and *Krt-2*. *J. Exp. Zool.* **263**: 83-95.
- Heid, H.W., E. Werner, and W.W. Franke. 1986. The complement of native alpha-keratin polypeptides of hair-forming cells: A subset of eight polypeptides that differ from epithelial cytokeratins. *Differentiation* **32**: 101-119.
- Heid, H.W., I. Moll, and W.W. Franke. 1988. Patterns of expression of trichocytic and epithelial cytokeratins in mammalian tissues II. Concomitant and mutually exclusive synthesis of trichocytic and epithelial cytokeratins in diverse human and bovine tissues (hair follicle, nail bed and matrix, lingual papilla, thymic reticulum). *Differentiation* **37**: 215-230.
- Holland, P.W.H. and J. Garcia-Fernandez. 1996. *Hox* genes and chordate evolution. *Dev. Biol.* **173**: 382-395.
- Kanzler, B., J.P. Viallet, H. Le Mouellic, E. Boncinelli, D. Duboule, and D. Dhouailly. 1994. Differential expression of two different homeobox gene families during mouse tegument morphogenesis. *Int. J. Dev. Biol.* **38**: 633-640.
- Kondo, T., P. Dollé, J. Zákány, and D. Duboule. 1996. Function of posterior *HoxD* genes in the morphogenesis of the anal sphincter. *Development* **122**: 2651-2659.
- Krumlauf, R. 1994. *Hox* genes in vertebrate development. *Cell*

- 7: 191–201.
- Lawrence, H.J., G. Sauvageau, R.K. Humphries, and C. Largman. 1996. The role of *HOX* homeobox genes in normal and leukemic hematopoiesis. *Stem Cells* **14**: 281–291.
- Lynch, M.H., W.M. O'Guin, C. Hardy, L. Mak, and T.-T. Sun. 1986. Acidic and basic hair/nail ("hard") keratins: Their localization in the upper cortical and cuticle cells of the human hair follicle and their relationship to "soft" keratins. *J. Cell Biol.* **103**: 2593–2606.
- Mann, S.J. 1962. Prenatal formation of hair follicle types. *Anat. Rec.* **144**: 135–142.
- Mansour, S.L., K.R. Thomas, and M.R. Capecchi. 1988. Disruption of the proto-oncogene *int-2* in mouse embryo-derived stem cells: A general strategy for targeting mutations to non-selectable genes. *Nature* **336**: 348–352.
- Mansour, S.L., K.R. Thomas, C. Deng, and M.R. Capecchi. 1990. Introduction of a *lacZ* reporter gene into the mouse *int-2* locus by homologous recombination. *Proc. Natl. Acad. Sci.* **87**: 7688–7692.
- Mansour, S.L., J.M. Goddard, and M.R. Capecchi. 1993. Mice homozygous for a targeted disruption of the proto-oncogene *int-2* have developmental defects in the tail and inner ear. *Development* **117**: 13–28.
- Matthews, C.H.E., K. Detmer, H.J. Lawrence, and C. Largman. 1993. The *hox 2.2* homeobox gene is expressed in epidermal tissue during murine embryogenesis. *Differentiation* **52**: 177–184.
- Mortlock, D.P. and J.W. Innis. 1997. Mutation of *HOXA13* in hand-foot-genital syndrome. *Nature Genet.* **15**: 179–180.
- Mortlock, D.P., L.C. Post, and J.W. Innis. 1996. The molecular basis of hypodactyly (*Hd*): A deletion in *Hoxa13* leads to arrest of digital arch formation. *Nature Genet.* **13**: 284–289.
- Nagy, A., J. Rossant, R. Nagy, W. Abramow-Newerly, and J.C. Roder. 1993. Derivation of completely cell culture-derived mice from early-passage embryonic stem cells. *Proc. Natl. Acad. Sci.* **90**: 8424–8428.
- Pendleton, J.W., B.K. Nagai, M.T. Murtha, and F.H. Ruddle. 1993. Expansion of the *Hox* gene family and the evolution of chordates. *Proc. Natl. Acad. Sci.* **90**: 6300–6304.
- Peterson, R.L., T. Papenbrock, M.M. Davda, and A. Awgulewitsch. 1994. The murine *Hoxc* cluster contains five neighboring *AbdB*-related *Hox* genes that show unique spatially coordinated expression in posterior embryonic subregions. *Mech. Dev.* **47**: 253–260.
- Pöpperl, H., M. Bienz, M. Studer, S.-K. Chan, S. Aparicio, S. Brenner, R.S. Mann, and R. Krumlauf. 1995. Segmental expression of *Hoxb-1* is controlled by a highly conserved autoregulatory loop dependent upon *exd/pbx*. *Cell* **81**: 1031–1042.
- Powell, B.C. and G.E. Rogers. 1990. Cyclic hair-loss and re-growth in transgenic mice overexpressing an intermediate filament gene. *EMBO J.* **9**: 1485–1493.
- . 1997. The role of keratin proteins and their genes in the growth, structure and properties of hair. In *Formation and structure of human hair* (ed. P. Jolles, H. Zahn, and H. Hocker), pp. 59–148. Birkhauser Verlag, Basel, Switzerland.
- Rieger, E., J.J. Bijl, J.W. van Oostveen, H.P. Soyer, C.B.M. Oudejans, N.M. Jiwa, J.M.M. Walboomers, and C.J.L.M. Meijer. 1994. Expression of the Homeobox gene *HOXC4* in keratinocytes of normal skin and epithelial skin tumors is correlated with differentiation. *J. Invest. Dermatol.* **103**: 341–346.
- Roberts, D.J., R.L. Johnson, A.C. Burke, C.E. Nelson, B.A. Morgan, and C. Tabin. 1995. Sonic hedgehog is an endodermal signal inducing *Bmp-4* and *Hox* genes during induction and regionalization of the chick hindgut. *Development* **121**: 3163–3174.
- Rogers, G.E. and B.C. Powell. 1993. Organization and expression of hair follicle genes. *J. Invest. Dermatol.* **101**: 50S–55S.
- Rothnagel, J.A. and D.R. Roop. 1995. Hair follicle companion layer: Reacquainting an old friend. *J. Invest. Dermatol.* **104**: 42S–43S.
- Scott, M.P. 1992. Vertebrate homeobox gene nomenclature. *Cell* **71**: 551–553.
- Sundberg, J.P. and M.E. Hogan. 1994. Hair types and subtypes in the laboratory mouse. In *Handbook of mouse mutations with skin and hair abnormalities* (ed. J.P. Sundberg), pp. 57–68. CRC Press, Boca Raton, FL.
- Thomas, K.R., C. Deng, and M.R. Capecchi. 1992. High-fidelity gene targeting in embryonic stem cells by using sequence replacement vectors. *Mol. Cell. Biol.* **12**: 2919–2923.
- Tobiasch, E., J. Schweizer, and H. Winter. 1992. Structure and site of expression of a murine type II hair keratin. *Mol. Biol. Rep.* **16**: 39–47.
- Winter, H., P. Siry, E. Tobiasch, and J. Schweizer. 1994. Sequence and expression of murine type I hair keratins mHa2 and mHa3. *Exp. Cell Res.* **212**: 190–200.
- Winter, H., M.A. Rogers, L. Langbein, H.P. Stevens, I.M. Leigh, C. Labrèze, S. Roul, A. Taieb, T. Krieg, and J. Schweizer. 1997. Mutations in the hair cortex keratin hHb6 cause the inherited hair disease monilethrix. *Nature Genet.* **16**: 372–374.
- Yokouchi, Y., J.-I. Sakiyama, and A. Kuroiwa. 1995. Coordinated expression of *Abd-B* subfamily genes of the *HoxA* cluster in the developing digestive tract of chick embryo. *Dev. Biol.* **169**: 76–89.
- Zappavigna, V., A. Renucci, J.-C. Izpisua-Belmonte, G. Urier, C. Peschle, and D. Duboule. 1991. *Hox4* genes encode transcription factors with potential auto- and cross-regulatory capacities. *EMBO J.* **10**: 4177–4187.
- Zeltser, L., C. Desplan, and N. Heintz. 1996. *Hoxb-13*: A new *Hox* gene in a distant region of the *HOXB* cluster maintains colinearity. *Development* **122**: 2475–2484.
- Zimmerman, F. and I.N. Rich. 1997. Mammalian Homeobox B6 expression can be correlated with erythropoietin production sites and erythropoiesis during development, but not with hematopoietic or nonhematopoietic stem cell populations. *Blood* **89**: 2723–2735.